E. J. W. Van Someren et al. (Eds.)
Progress in Brain Research, Vol. 193
ISSN: 0079-6123

CHAPTER 18

Modulation of the brain's functional network architecture in the transition from wake to sleep

Linda J. Larson-Prior[†,*], Jonathan D. Power[‡], Justin L. Vincent[§], Tracy S. Nolan[†], Rebecca S. Coalson[†,‡], John Zempel[‡], Abraham Z. Snyder[†,‡], Bradley L. Schlaggar[†,‡,¶,‖], Marcus E. Raichle[†,‡,¶,#] and Steven E. Petersen[†,‡,¶,**]

[†] *Washington University in St. Louis, Mallinckrodt Institute of Radiology, Neuroimaging Laboratory, St. Louis, MO, USA*
[‡] *Department of Neurology, Washington University School of Medicine, St. Louis, MO, USA*
[§] *Harvard University, Center for Brain Science, Cambridge, MA, USA*
[¶] *Department of Anatomy and Neurobiology, Washington University School of Medicine, St. Louis, MO, USA*
[‖] *Department of Pediatrics, Washington University School of Medicine, St. Louis, MO, USA*
[#] *Department of Biomedical Engineering, Washington University School of Engineering, St. Louis, MO, USA*
[**] *Department of Psychology, Washington University, St. Louis, MO, USA*

Abstract: The transition from quiet wakeful rest to sleep represents a period over which attention to the external environment fades. Neuroimaging methodologies have provided much information on the shift in neural activity patterns in sleep, but the dynamic restructuring of human brain networks in the transitional period from wake to sleep remains poorly understood. Analysis of electrophysiological measures and functional network connectivity of these early transitional states shows subtle shifts in network architecture that are consistent with reduced external attentiveness and increased internal and self-referential processing. Further, descent to sleep is accompanied by the loss of connectivity in anterior and posterior portions of the default-mode network and more locally organized global network architecture. These data clarify the complex and dynamic nature of the transitional period between wake and sleep and suggest the need for more studies investigating the dynamics of these processes.

Keywords: sleep; functional connectivity; graph theory; brain networks; alpha EEG; fMRI; EEG/fMRI.

*Corresponding author.
Tel: 1-314-362-7318
E-mail: lindap@npg.wustl.edu

DOI: 10.1016/B978-0-444-53839-0.00018-1

Introduction

Sleep represents a series of well-defined and behaviorally relevant transitions in neural state that are stable across normal human sleepers while showing distinct changes across the lifespan (Campbell and Murphy, 2007; Gertner et al., 2002; Munch et al., 2010; Terry et al., 2004) and in many neuropathologies (Claassen et al., 2010; Moller et al., 2009; Song et al., 2010; Walters et al., 2008). While a number of studies have examined network correlates of stable NREM (Braun et al., 1997; Czisch et al., 2004; Dang-Vu et al., 2005, 2008; Horovitz et al., 2008, 2009; Kaufmann et al., 2006; Larson-Prior et al., 2009; Nofzinger et al., 2002; Spoormaker et al., 2010) and REM (Braun et al., 1997; He et al., 2008; Magnin et al., 2004; Maquet et al., 1996, 2005; Wehrle et al., 2005, 2007) sleep, far fewer have examined those of the initial transitional stage of sleep (N1; Corsi-Cabrera et al., 2006; Jann et al., 2009; Kjaer et al., 2002; Laufs et al., 2006; Olbrich et al., 2009; Picchioni et al., 2008). Yet it is in this initial period that the brain progressively disengages from the external world. Investigation of the neural network correlates of this state, in which the individual may either transition to stable sleep or return to wakefulness, may provide insights into pathological conditions characterized by instability in external versus internal awareness (cognitive fluctuations, Escandon et al., 2010; narcolepsy, Zorick et al., 1986; sundowning, Bachman and Rabins, 2006; sleep attacks in Parkinson's disease, Moller et al., 2009).

Human sleep is defined by characteristic changes in the scalp-recorded electroencephalogram (EEG). From an initial state of quiet waking the individual begins to transition to a more inwardly directed state accompanied by eye closure and broadly characterized by the presence of low frequency oscillatory potentials in posterior cortex (alpha band, 8–12 Hz). During quiet wakefulness, subjects slowly oscillate between attending to external and internal thoughts, with the majority of internal thoughts being autobiographical or self-referential in nature (Andrews-Hanna et al., 2010b; Vanhaudenhuyse et al., 2010). Further, these internally directed spontaneous thoughts are strongly related to activity in major elements of the default-mode network (DMN; Andrews-Hanna et al., 2010a; Mason et al., 2007; Vanhaudenhuyse et al., 2010).

Because alpha-band oscillatory activity characterizes quiet wakefulness, a number of studies have investigated its neural correlates using simultaneously acquired functional magnetic resonance imaging (fMRI) and EEG (de Munck et al., 2007; Goldman et al., 2002; Goncalves et al., 2006; Jann et al., 2009; Laufs et al., 2003a,b; Moosmann et al., 2003; Sadaghiani et al., 2010; Tyvaert et al., 2008). The relationship of alpha-band power and the blood oxygen-level dependent (BOLD) signal of fMRI exhibit a general pattern in which thalamus shows positively correlated activity, while frontoparietal and occipital regions exhibit anticorrelated activity. Together with studies reporting reduced attention to the external environment, these correlations suggest a reduction of activity in brain regions associated with externally directed attention and a potential increase in activity in the DMN, which is generally considered to be related to inwardly directed awareness (Andrews-Hanna et al., 2010a; Gusnard et al., 2001; Vanhaudenhuyse et al., 2010). Yet there remain significant differences in reported positive alpha-band correlations to elements of the DMN (Ben-Simon et al., 2008; Jann et al., 2009; Laufs et al., 2003b), and no study reporting positive correlations to all of the core elements of this network.

Sleep onset (N1) is defined by the loss of posterior alpha-band activity, general slowing of the EEG with prominent theta-band (4–7 Hz) activity, and slow rolling eye movements (Iber et al., 2007). N1 is a transitional state and frequently exhibits brief alpha bursts and arousals (Davis et al., 1938; Ogilvie, 2001) prior to attaining

"true" early non-rapid eye-movement (NREM) sleep (N2). Because of its transitional nature, the features defining N1 as a discrete stage of sleep have been a matter of debate (Corsi-Cabrera et al., 2006; De Gennaro et al., 2005; Merica and Fortune, 2004; Ogilvie, 2001; Roth, 1961), with some suggesting that sleep onset would better be defined by the presence of EEG features unique to N2 (K-complexes and sleep spindles: Ogilvie, 2001; Merica and Fortune, 2004). The reduced responsiveness to external stimulation in N1 sleep has also been investigated using electrical potentials evoked by auditory stimuli (see Atienza et al., 2001 for review). Studies investigating the relationship of EEG rhythms to cognitive activity in N1 sleep (Atienza et al., 2001; Cicogna et al., 1998; Rowley et al., 1998; Yang et al., 2010), report that behavioral and electrophysiological responses to external stimuli drop significantly while internal thought content continues to focus on daily experiences and life concerns.

A small number of studies have addressed regional changes in brain activity during N1 sleep (Kaufmann et al., 2006; Kjaer et al., 2002; Olbrich et al., 2009; Picchioni et al., 2008). Reduced activity in frontoparietal cortices and thalamus has been reported for N1 relative to wake (Kaufmann et al., 2006; Kjaer et al., 2002). When N1 is separated into substates (Picchioni et al., 2008), early N1 was associated with increased BOLD activity in frontal cortices and extend to temporal (Olbrich et al., 2009) and parietal (Picchioni et al., 2008) regions while in late N1 a distinctly different pattern with a more posterior distribution of activity was reported. This shift has been attributed to a transient increase in default-mode network activity in early N1 sleep related to decreases in externally directed cognition (Picchioni et al., 2008).

Following N1, stable sleep is established during which NREM (N2 and N3) and rapid eye-movement (stage REM) sleep rhythmically alternate for 2–7 cycles over night in normal sleepers. N2 is associated with further reductions in the perception of external stimuli (Yang et al., 2010). N2 exhibits reduced electrophysiological and fMRI responsiveness to external stimulation (Czisch et al., 2004; Portas et al., 2000). In addition, relative to quiet wakefulness, BOLD signal decreases in N2 have been reported in brain regions activated by task performance in the waking state (Kaufmann et al., 2006).

Given the association between DMN activity and inwardly directed cognition, the reduction in activity in large frontoparietal regions generally associated with externally directed awareness, and the anticorrelated nature of default and attention-related network activity (Fox et al., 2005), a number of studies have investigated potential shifts in the functional connectivity of these networks (Horovitz et al., 2008, 2009; Larson-Prior et al., 2009) in early NREM sleep. In all cases, core members of both DMN and attentional networks retained their interregional connectivity during light sleep. However, with the deepening of sleep (N3, slow wave sleep), medial prefrontal regions of the DMN decouple from posterior elements (Horovitz et al., 2009) while posterior elements show strengthened connectivity. A recent study using graph theoretical approaches to investigate network changes in sleep reports that light NREM (N1/N2) sleep exhibits a general increase in corticocortical connectivity that weakens with the onset of N3 (Spoormaker et al., 2010) consistent with reported strengthening of visual and somatomotor (SM) regions (Horovitz et al., 2009) and dorsal attention regions (Larson-Prior et al., 2009) reported by others in N2.

There is general agreement that the descent to sleep is accompanied subjectively by reduced awareness of the external world and objectively by reduced responsiveness to stimuli; however, the changes in brain network architecture that presumably underlie this remain unclear. The extant literature provides a somewhat confusing picture of the functional changes associated with disengagement. On the one hand, mind-wandering in quiet wake has been associated with

increased activity in the DMN (Andrews-Hanna et al., 2010a; Mason et al., 2007; Vanhaudenhuyse et al., 2010). On the other hand, imaging studies in quiet wake report a general decrease in activity in a broad frontoparietal network with no increase in DMN activity (Kaufmann et al., 2006; Laufs et al., 2006).

This report seeks to add to our understanding of the neural network changes that accompany the early descent to sleep. We present two types of result: (1) alpha-BOLD correlations related to sleep stage and (2) BOLD–BOLD correlations in different stages of sleep. BOLD–BOLD correlation analyses include both conventional, seed-based correlation mapping and a graph theoretical approach making no *a priori* assumptions about the functional network membership of the ROIs evaluated to define changes in network architecture (Bullmore and Sporns, 2009; Humphries and Gurney, 2008; Power et al., 2010b; Watts and Strogatz, 1998).

Methods

General methods

Subjects

Sixty-seven right-handed, healthy human subjects were recruited from the campus of Washington University under two study protocols approved by the University's Human Studies Committee. Both studies acquired EEG and fMRI simultaneously. Fifty-seven subjects were asked to lie quietly with eyes closed and remain awake (Group 1). Ten subjects were recruited to a study in which they were asked to sleep in the scanner (Group 2; see Larson-Prior et al., 2009 for details).

Twenty-four subjects (11 female) comprised the Group 1 analysis set (27 had bad or incomplete data and 6 withdrew early). Six subjects in Group 2 (4 female) provided artifact-free data that contained polysomnographically verified early stage NREM sleep (see Larson-Prior et al., 2009 for details). Group 1 provided 3 × 5 min (short scans) and 1–20 min eyes-closed resting state scans (long scan), while Group 2 provided six data sets that included stable NREM sleep (14.7–37.6 min in duration). Following rejection for excessive movement or poor EEG signal quality, data from 24 short (3 × 5 min) and 21 long (20 min) data sets in Group 1 were submitted to analysis.

Functional imaging

Whole brain fMRI BOLD (Siemens Allegra 3T scanner; Erlangen, Germany; TE = 30 ms, 4 mm^3 voxels, 2.013 s per volume, 1 s pause between frames) was acquired using an EPI sequence locally modified to enhance the signal/noise ratio. Structural data used for atlas transformations included a high-resolution (1 × 1 × 1.25 mm) sagittal, T1-weighted magnetization-prepared rapid gradient-echo scan.

Image preprocessing

FMRI data preprocessing included compensation of slice-dependent time shifts and elimination of intensity differences, rigid body correction for head motion, intensity scaling (to obtain a whole brain mode value of 1000), and atlas registration by affine transformation (Ojemann et al., 1997). Runs were transformed to atlas space and resampled to 3 mm^3 voxels in a Talairach coordinate frame. Seed-based functional connectivity analyses were performed as previously described (Fox et al., 2005; Larson-Prior et al., 2009). Briefly, following regression of noise signals, 10 mm diameter seed regions of interest (ROI) were centered in the posterior cingulate/precuneus region (PCC; Talairach coordinates −2, −36, +3) for the DMN, in the right intraparietal sulcus (RIPS; Talairach coordinates 25, −58, 52) for the dorsal attention network

(DAN), and in right frontal operculum (RfOP; Talairach coordinates −35, 14, 5) for the executive control network (ECN). The BOLD time series from each ROI was extracted and correlated to all other brain voxels to produce both ROI–ROI correlation matrices and spatial correlation maps. Results were calculated as Fisher-z transformed correlation values and spatial group data were evaluated using a fixed effects analysis ($p < 0.05$, corrected for multiple comparisons). For hypothesis testing, correlation values across the three attention networks evaluated (DMN, DAN, and ECN) were evaluated by pairwise Student's *t*-tests.

Electroencephalography

FMRI and EEG were collected simultaneously (DC-3500 Hz, 20 KHz sampling rate) using the MagLink™ (Compumedics Neuroscan, TX) system and the Synamps/2™ amplifier. 64 EEG sensors were recorded from an extended 10–20 system (MagLink™ cap including bipolar vertical eye leads, bipolar EKG leads, and two ear leads, reference electrode 5 cm posterior to CZ). An external cardiac lead (InVivo Research Inc., FL) was recorded for use in off-line artifact correction. Gradient artifact was reduced using Scan 4.5 software (filtered 1–30 Hz and downsampled to 500 Hz). Gross motion artifacts in the EEG were visually scored by an experienced electroencephalographer (JZ) and removed prior cardiac artifact (ballistocardiogram, BKG) correction using an algorithm developed in our laboratory (Vincent et al., 2007; Group 1). For sleep subjects (Group 2), BKG was reduced using ICA-based algorithm and the Curry 6.0 software package (Compumedics Neuroscan, TX), after which data were visually scored for sleep stage in 30 s intervals by an experienced electroencephalographer (JZ) according to standard criteria (Rechtsaffen and Kales, 1968; Iber et al., 2007; for further details see Larson-Prior et al., 2009).

Data processing and analysis

Correlation of electrophysiological and fMRI BOLD resting state network activity

Following preprocessing of EEG, alpha (8–12 Hz) band signal was extracted from an occipital electrode (O1) and power spectral density was calculated in 2.048 second time bins. The alpha power time series was convolved with a canonical hemodynamic response model (Boyton et al., 1996) to provide a time series (αHDR) of alpha-band power filtered to the frequency of the BOLD time signal. αHDR was correlated to BOLD signal for each subject in a voxel-wise manner for both short and long data sets. Data were subject to both fixed ($p < 0.05$, corrected) and random effects ($p < 0.01$, uncorrected) analyses. All data are displayed for fixed effects, and differences between statistical maps under this regime and those examined using a random effects analysis are noted in the text.

To assess possible state variability, spectral power in the alpha (8–12 Hz) and theta (4–7.5 Hz) bands was computed by FFT (1 s time bins) for occipital electrode derivations (O1 and O2). To identify scans with shifts in neural state from alert wake in Group 1 subjects, a hierarchical cluster analysis was performed. Six parameters were computed to characterize band-limited power time series: the ratio of the total alpha and theta power (ATR), the first four moments of the alpha power time series (M1–M4), and the coefficient of variation ($C_v = \sigma_{A'}/\mu_A$) of the αHDR. Principle components and pairwise correlation analyses were used to reduce the dimensionality of the problem. ATR and M2 (variance) were found to partition the data into the same two identifiable clusters that resulted from the analysis of the full parameter set. One way analysis of variance (ANOVA) of M2 and ATR was computed for both 5 and 20 min data sets. Pairwise differences between the two clusters were tested using a Wilcoxon rank sums test, and are significant for both ATR ($p = 0.001$)

and M2 ($p = 0.0022$) for 5 min data sets and for M2 ($p = 0.001$) in 20 min data sets. Statistical analyses were performed using JMP 7.0 (SAS Institute, Inc.). Based on these results, data were partitioned into two groups: (1) alert wake (9 subjects, 27 5-min data runs; 5 20-min data runs) and (2) transition to sleep (N1 sleep; 16 subjects, 44 5-min data runs, 17 20-min data runs). No Group 1 subject attained stage 2 NREM sleep. Five minute data sets were analyzed as concatenated 15 min (short) runs in which assignment was based on the predominant sleep stage over the 3 runs.

Large-scale network analysis—Seed region definition One hundred and fifty-one ROI (Table 1) were defined on the basis of task-induced BOLD activations (Power et al., 2010a) acquired on the same Siemens 1.5 Tesla Vision scanner. A series of eight meta-analyses (Dosenbach et al., 2006), focused on error-processing, positive sustained activity, task-induced deactivations (default-mode), memory, language, and sensorimotor functions were combined with previously published cognitive control regions (Dosenbach et al., 2007; Fair et al., 2007) to create a conjunction image, where each voxel carried a value between zero and the number of studies in which that voxel was significant. A peak-finding algorithm identified centroids of reliably activated groups of voxels at least 10 mm apart (see Dosenbach et al., 2010 for details). Ten millimeters diameter spherical volumes were centered on these peaks to define 151 non-overlapping seed ROIs that were then used to seed our resting state data sets (Fig. 3).

Large-scale analysis of network changes from wake to sleep To examine this large data set, we chose a graph theoretic approach (Fair et al., 2009; Power et al., 2010b). Time series were extracted for the 151 seed regions from each resting state data series (Group 1 short and long runs and Group 2). Correlation values were calculated on these time series between each seed and all other regions to create a set of square matrices (151×151). Data sets were assigned based on a hierarchical cluster analysis performed on band-limited EEG data (wake and N1) or on the presence of K-complexes and sleep spindles (N2) and correlation matrices were averaged across data sets for each group. For graph analysis, the seed regions were considered nodes and the edges were defined on the basis of the correlation between connected nodes.

Community structure analysis Like many other complex networks, the brain is organized into sets of modules (communities) which are represented graphically as a set of nodes whose within-group connectivity is greater than their between-group connectivity (Bullmore and Sporns, 2009; Fair et al., 2009; Lancichinetti et al., 2010; Power et al., 2010b). To evaluate network community structure, we chose the measure of network modularity (Q) developed by Newman (Newman, 2006). Optimizing modularity, subgroups are calculated by an iterative algorithm that divides a network into groups with as many within-group connections and as few between group connections as possible. The value of modularity (Q) for the whole network should be at least 0.3 (Newman, 2006) for networks with hundreds of elements; we chose $Q = 0.4$ as a conservative lower bound.

It is important to examine a range of thresholds over which the density of connections (edge density) between seed regions (nodes) varies from dense (low thresholds) to more sparse (high thresholds) for each subject group. After examining network densities on the region/correlation graphs over a range of positive correlation thresholds, the threshold at which average edge density (k_{den}) was equal to the natural logarithm of the number of nodes ($\ln N$) was chosen as the upper bound in accord with previous graph theoretical studies. Threshold ranges were assigned on the basis of graph network metrics (lowest threshold at $Q = 0.4$, highest threshold at $k_{\mathrm{den}} = 5 = \ln(151)$) for each group (In steps of 0.01: 0.08–0.26 awake; 0.06–0.25 N1, 0.11–0.31 N2).

Table 1. Tailarach coordinates and anatomical location of seed regions of interest

ROI	X	Y	Z	Anatomical location	Net
1	−10	−21	8	L Thalamus	C-O
2	−11	−57	14	L Post Cing	DMN
3	−12	−41	1	L PHG	P-O
4	−15	−53	−2	L Occipital	P-O
5	−15	−65	−20	L Cerebellum	CbA
6	−15	0	10	L Int Capsule	C-O
7	−16	−75	−25	L Cerebellum	CbA
8	−16	−77	30	L Occipital	P-O
9	−17	−68	3	L Occipital	P-O
10	−17	23	54	L Frontal	DMN
11	−1	−18	46	L Frontal	SM
12	−1	25	30	L Cingulate	C-O
13	−21	−34	58	L Parietal	SM
14	−21	4	−2	L Putamen	C-O
15	−25	−41	−8	L PHG	DMN
16	−25	−89	0	L Occipital	P-O
17	−26	−71	33	L Parietal	F-P
18	−27	−79	16	L Occipital	P-O
19	−27	46	25	L Frontal	C-O
20	−28	−59	44	L Parietal	F-P
21	−29	−29	12	L Sublobar	SM
22	−2	−16	13	L Thalamus	C-O
23	−2	10	45	L Frontal	C-O
24	−30	−14	1	L Putamen	C-O
25	−30	−55	−25	L Cerebellum	CbA
26	−31	−78	−15	L Occipital	P-O
27	−32	−48	44	L Parietal	F-P
28	−32	−5	53	L Frontal	F-P
29	−33	0	6	L Claustrum	C-O
30	−33	49	9	L Frontal	F-P
31	−34	16	3	L Insula	C-O
32	−37	−35	16	L Temporal	SM
33	−39	−22	52	L Parietal	SM
34	−39	−75	22	L Occipital	DMN
35	−3	−37	30	L Cingulate	DMN
36	−3	−39	42	L Cingulate	DMN
37	−3	−50	12	L Post Cing	DMN
38	−3	−81	18	L Occipital	P-O
39	−3	32	39	L Frontal	F-P
40	−3	36	20	L Ant Cing	DMN
41	−3	39	−4	L Ant Cing	DMN
42	−40	−60	−10	L Occipital	P-O
43	−40	−73	−2	L Occipital	P-O
44	−40	2	33	L Frontal	F-P
45	−40	40	2	L Frontal	F-P
46	−41	−56	41	L Parietal	F-P
47	−41	20	31	L Frontal	F-P
48	−43	−2	45	L Frontal	F-P
49	−43	−3	10	L Insula	SM
50	−43	−65	31	L Parietal	DMN
51	−44	−34	44	L Parietal	SM
52	−44	−61	18	L Temporal	DMN
53	−45	7	24	L Frontal	F-P
54	−47	−28	5	L Temporal	C-O
55	−47	−43	0	L Temporal	Sw
56	−47	21	2	L Frontal	Sw
57	−48	−14	34	L Frontal	SM
58	−48	−36	24	L Parietal	SM
59	−49	5	0	L Insula	C-O
60	−4	−2	53	L Frontal	C-O
61	−4	21	46	L Frontal	F-P
62	−51	−13	24	L Parietal	SM
63	−51	−24	22	L Parietal	SM
64	−51	−50	39	L Parietal	F-P
65	−52	−25	41	L Parietal	SM
66	−53	−41	12	L Temporal	SM
67	−54	−51	8	L Temporal	Sw
68	−55	−27	−14	L Temporal	DMN
69	−55	−31	−4	L Temporal	Sw
70	−58	−27	13	L Temporal	SM
71	−5	−30	−3	L Midbrain	C-O
72	−6	13	36	L Cingulate	C-O
73	−7	−56	25	L Post Cing	DMN
74	−7	−72	38	L Precuneus	DMN
75	−7	45	4	L Ant Cing	DMN
76	−8	−68	29	L Precuneus	DMN
77	−8	−80	5	L Occipital	P-O
78	10	−55	16	R Post Cing	DMN
79	10	−67	39	R Parietal	DMN
80	11	−20	9	R Thalamus	C-O
81	14	−64	24	R Occipital	DMN
82	14	−77	28	R Occipital	P-O
83	14	1	10	R Int Capsule	C-O
84	17	−79	−34	R Cerebellum	CbB
85	18	−32	58	R Frontal	SM
86	19	−66	1	R Occipital	P-O
87	19	−85	−4	R Occipital	P-O
88	1	−27	30	R Cingulate	DMN
89	1	−31	58	R Parietal	SM
90	1	−62	−18	R Cerebellum	CbA

(*Continued*)

Table 1. (*Continued*)

ROI	X	Y	Z	Anatomical location	Net
91	21	27	50	R Frontal	DMN
92	22	–58	–22	R Cerebellum	CbA
93	22	6	5	R Lentiform	C-O
94	24	43	31	R Frontal	C-O
95	25	–79	–16	R Occipital	P-O
96	26	–39	–11	R PHG	DMN
97	27	–3	7	R Lentiform	C-O
98	27	–77	23	R Occipital	P-O
99	28	–76	–31	R Cerebellum	CbB
100	29	–17	4	R Lentiform	C-O
101	29	27	30	R Frontal	C-O
102	29	49	20	R Frontal	C-O
103	30	–29	14	R Extranuclear	SM
104	31	–55	42	R Parietal	F-P
105	32	12	–3	R Insula	C-O
106	34	–13	16	R Insula	SM
107	34	–67	–33	R Cerebellum	CbB
108	34	17	7	R Insula	C-O
109	34	6	5	R Insula	C-O
110	35	–3	0	R Insula	C-O
111	35	–66	38	R Parietal	F-P
112	35	–81	0	R Occipital	P-O
113	35	–84	11	R Occipital	P-O
114	36	37	20	R Frontal	F-P
115	37	13	42	R Frontal	F-P
116	38	–73	13	R Occipital	P-O
117	39	–24	54	R Parietal	SM
118	39	–5	48	R Frontal	C-O
119	3	–50	48	R Parietal	DMN
120	40	–66	–8	R Occipital	P-O
121	41	–26	21	R IPL	SM
122	41	–55	45	R Parietal	F-P
123	41	–73	26	R Occipital	DMN
124	41	43	4	R subgyral	F-P
125	44	–52	28	R TPJ	DMN
126	44	–60	4	R Occipital	P-O
127	44	5	35	R Frontal	F-P
128	45	17	14	R Frontal	C-O
129	45	19	30	R Frontal	F-P
130	46	–45	44	R Parietal	F-P
131	47	4	3	R Precentral	C-O
132	48	–10	34	R Frontal	SM
133	49	–31	–2	R Temporal	Sw
134	49	–35	9	R Temporal	SM
135	49	–61	34	R Parietal	DMN
136	4	18	39	R Cingulate	C-O
137	51	–31	34	R Parietal	SM
138	51	–45	22	R TPJ	Sw
139	52	–47	36	R Parietal	F-P
140	53	–33	–14	R Temporal	DMN
141	53	–48	12	R Temporal	Sw
142	53	–9	16	R Parietal	SM
143	55	–19	10	R Temporal	SM
144	6	–26	1	R Thalamus	C-O
145	6	–81	4	R Occipital	P-O
146	7	–50	29	R Cingulate	DMN
147	7	37	0	R Ant Cing	DMN
148	8	–72	9	R Occipital	P-O
149	8	–7	8	R Thalamus	C-O
150	9	–41	48	R Parietal	SM
151	9	17	30	R Cingulate	C-O

Network	Color	Name	Abbreviation
1	Orange	Switching	Sw
2	Green	Parietal Occipital	P-O
3	Black	Cingulo-Opercular	C-O
4	Red	Default	DMN
5	Yellow	Fronto-Parietal	F-P
6	Pink	Somato-Motor	SM
7	Blue	CerebellarA	CbA
8	Purple	Cerebellar B	CbB

PHG = Parahippocampal gyrus
Cing = cingulate gyrus
TPJ = temporal parietal junction
IPL = inferior parietal lobule

Based on community detection analyses over these thresholds, a new 151 × 151 matrix was formed in which the value for each pair of nodes was the proportion of thresholds in which two regions were assigned to the same subgroup. Final region groupings were objectively assigned by the weighted modularity algorithm on these proportions at a threshold of 60% same subgroup assignment (thresholds from 0% to 75% were examined for consistency of assignment).

SoNIA visualization To visualize the shifts in global network architecture occurring with changing neural state, we used a spring embedding algorithm that is helpful in qualitative interpretation of the structures of large-scale networks (see Fair et al., 2009; Power et al., 2010b for further details). All computations were performed using MATLAB (the Mathworks, Natick, MA) and SoNIA (Social Network Image Animator; Bender-deMoll and McFarland, 2006).

PALS visualization mapping CARET brain mapping software (http://brainmap.wustl.edu/caret, Van Essen et al., 2001) and the PALS human cortical atlas (Van Essen, 2005) were used to create display maps for both αHDR correlation statistical images and region of interest locations for graph analyses.

Results

Alpha-band EEG and rsfMRI correlations

Correlation maps between the alpha power time series and simultaneously acquired fMRI exhibited distinctly different patterns dependent on the scan duration (Fig. 1). Short runs (Fig. 1a) demonstrated a pattern of positive correlations to PCC, medial prefrontal cortex (mPFC)/anterior cingulate, and right lateral parietal cortex. Anticorrelated activity was seen bilaterally in the superior parietal lobule (SPL), diffusely along the intraparietal sulcus (IPS), and in medial premotor cortex, all of which are elements of the DAN (Corbetta and Shulman, 2002; Fox et al., 2006), and in lateral frontal regions associated with the frontoparietal control system identified in both task and resting states (Dosenbach et al., 2007; Vincent et al., 2008). Over long scan durations (Fig. 1b), the pattern shifted to one in which midcingulate regions are most strongly correlated to αHDR and correlations to PCC were lost. Positive correlations to αHDR were apparent in the anterior insula/fronto-opercular (aI/fOp) region bilaterally and along the parietal–temporal border, more strongly on the left. Negative correlations of αHDR and BOLD became prominent bilaterally in the DAN, bilateral dorsolateral and inferior frontal cortex, right anterior superior temporal cortex, middle and inferior temporal cortex, and lateral visual areas.

Several laboratories have reported a positive correlation of alpha band to BOLD activity in the thalamus (de Munck et al., 2007; Feige et al., 2005; Goldman et al., 2002; Goncalves et al., 2006; Moosmann et al., 2003; Tyvaert et al., 2008) during quiet eyes-closed waking. We also saw positive correlations of alpha-band power to medial thalamic regions in both long and short data sets. Positive correlation of alpha-band activity and BOLD to medial thalamic regions, and a lack of correlation to visual thalamus or pulvinar have also been reported by others during quiet rest (Feige et al., 2005).

Small-scale network connectivity analysis

Group 1 data sets were assigned to either wake or N1 states based on the results of a hierarchical cluster analysis, with N2 derived from Group 2 data sets (6 subjects, 2892 frames; see Table 1 in Larson-Prior et al., 2009 for further details). We compared the correlation matrices of three attention-related networks (DMN (PCC), DAN (R-IPS), and an ECN (fOP)) across arousal states. Figure 2 illustrates the results of this analysis, showing reduced anticorrelations between DMN and both DAN and ECN across state. These

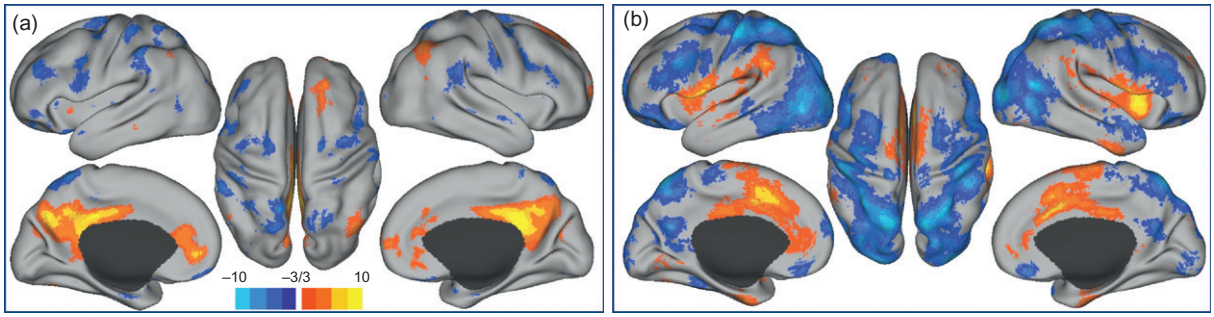

Fig. 1. αHDR to BOLD correlations. (a) Data are illustrated over 5 min duration runs (3/subject, 24 subjects). (b) Data are illustrated over 20 min duration runs (1/subject, 21 subjects). In color figures, hot colors represent positive correlations, while cool colors indicate anticorrelated activity. Statistical maps are shown for a fixed effects analysis corrected for multiple comparisons ($p < 0.05$).

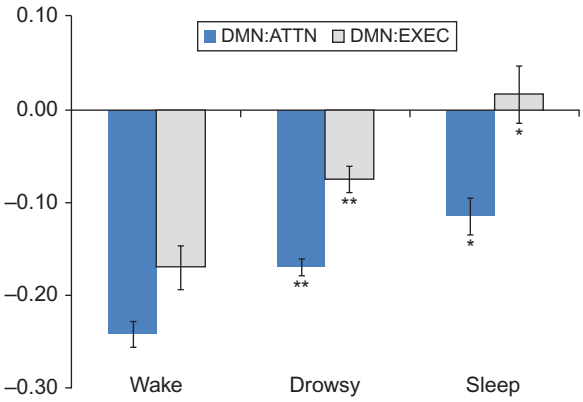

Fig. 2. A hallmark of the descent to sleep is the reduction in functional anticorrelations between core regions of the default mode network and those of dorsal attention and executive control networks. $^{**}p < 0.001$ and $^{*}p < 0.05$.

observed shifts in network connectivity during the descent to sleep are consistent with behavioral data; however, these results are framed in terms of ROI-voxel correlations, which provides a limited view of network reorganization.

Large-scale network connectivity analysis

To obtain a more comprehensive view of shifts in functional network connectivity in the transitional states from wake to sleep, we evaluated a large-scale network (Table 1; Fig. 3) where seed ROIs were derived from task-based fMRI studies (Dosenbach et al., 2006; Power et al., 2010a), using graph theoretical analysis techniques.

A hallmark of many real-world complex systems is a small-world network topology as defined in the seminal paper of Watts and Strogatz (1998). Recently, Humphries and Gurney (2008) defined a precise measure of small-worldness in networks (S) that quantifies this property, where $S > 1$ defines a network as small-world. As has been reported by others (Spoormaker et al., 2010), the networks examined here exhibited small-world properties in all three arousal states (wake: $S = 3.82$, N1: $S = 3.89$, N2: $S = 4.17$ at threshold $Q = 0.4$). While network metrics were generally similar between wake and N1, in N2 sleep an increase in edge density across thresholds indicated an general increase in network connectedness.

Modularity analysis revealed a robust community structure that was strongly associated with functional networks identified in both task (Beauchamp et al., 2001; Dosenbach et al., 2006; Esposito et al., 2006) and resting state (De Luca et al., 2006; Dosenbach et al., 2007; Fox et al., 2005) studies (Fig. 4). In the waking state, a set

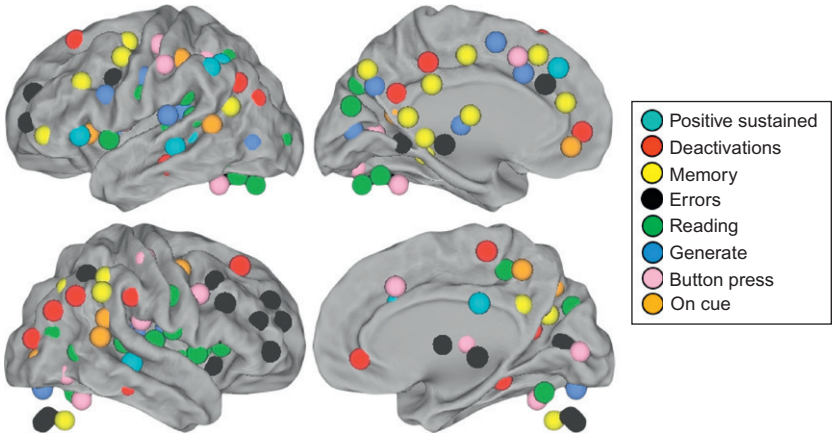

Fig. 3. Map of regions used in global network analysis of the transitional states from wake to sleep are illustrated as spheres centered on the coordinates for 151 regions of interest derived from a meta-analysis of task fMRI studies. Spheres are illustrated larger than 10 mm for ease of visualization. The legend indicates the meta-analysis task region nearest the combined region illustrated.

of strongly connected regions could be seen to segregate to cerebellum, SM, frontoparietal (FPS), cingulo-opercular (COPs), parieto-occipital (POS), and default-mode (DMN) systems, in addition to an independent module associated with task-switching (TSw; Fig. 4). The TSw network was comprised of six temporal and one fOp region related to the same task function (positive sustained; Dosenbach et al., 2006).

In N1, temporal TSw regions shifted their association to the sensorimotor system, while the frontal opercular region, which had connected the COPs to the TSw, joined the COPs. This set of regions further reconfigured in N2 and joined the FPS (Fig. 5). The remaining changes occurring in N1 sleep are seen in single regions or small region clusters. Thus, shifts in network architecture from wake to N1 are not global, but tend toward consolidation of smaller, task-related networks into larger and more loosely connected networks.

In N2 there is a shift in network architecture that biases networks toward more local, near-neighbor connection patterns. Interestingly, this was particularly strong for the anterior (mPFC) and posterior (PCC and lateral parietal) components of the DMN, which lose their identity as a single sub-network in this stage of sleep (Fig. 5). This dissociation is due to a significant weakening of inter-regional connectivity, with anterior elements of the wake state DMN showing reduced correlation to both posterolateral ($p = 0.001$) and posteromedial ($p < 0.001$) regions. In addition, as has been reported by others (Horovitz et al., 2009), there was a general strengthening of the correlation between individual nodes in the posteromedial DMN ($r_{avg} \pm$SEM, wake: 0.32 ± 0.03, N2: 0.36 ± 0.03). Further, each subregion in the DMN (posteromedial, anteromedial and lateral) associated with larger networks to which they were anatomically more related (Fig. 5). The dissociation between anterior and posterior nodes of the DMN was predominantly driven by the loss of their inter-regional connectivity, although some increase in the correlation of these nodes to the networks with which they associate in N2 was seen.

The FPS enlarged in N2 to include posterior members of the DMN, and lateral temporal regions. The POS captures those regions

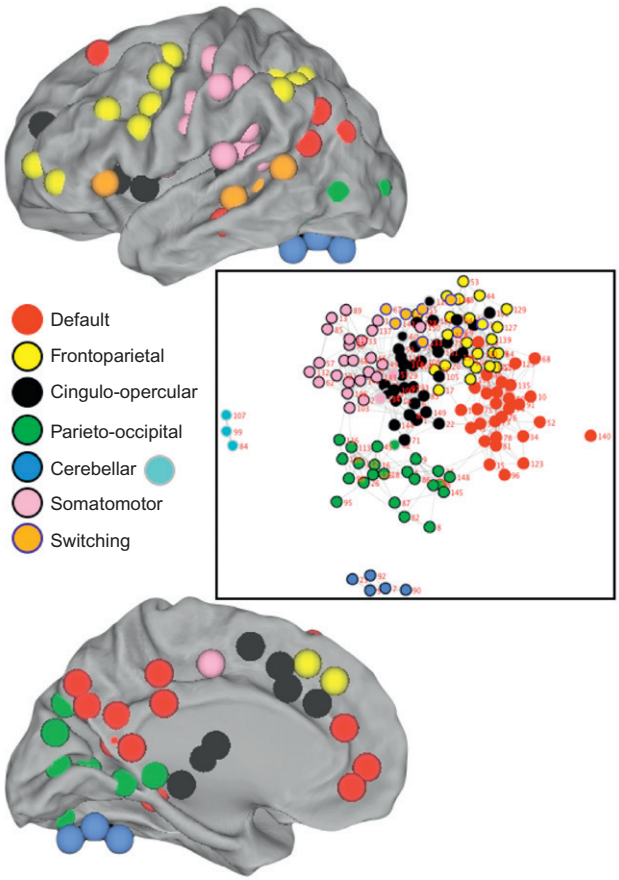

Fig. 4. Community structure in the wake state global network architecture. CARET maps show the communities to which each of 151 regions of interest were assigned. Notably, regions segregate into communities whose anatomical locations are consistent with a set of neural networks (legend) defined both on task and resting state fMRI. The central map illustrates community structure using the SoNIA visualization tool based on modularity analysis of global network structure. Subnetwork connectedness and the degree to which each community segregates from others in the network can be seen using this tool.

comprising the posterior components of the DMN for whom a parahippocampal node (node 3) is associated as a connector (Fig. 5). Four mPFC regions associated with DMN in wake, shift their association to the COPs in N2 sleep (Fig. 5).

Five thalamic ROIs were included in our data set. Interestingly, all of these regions grouped with the COPs in all three alertness states examined. The two thalamic regions with the strongest node degrees were also connected to each other in all three states, and the overall correlation between thalamic ROIs strengthened from wake to N2 ($r_{avg} \pm$SEM, wake, 0.47 ± 0.06; N1, 0.51 ± 0.06; N2, 0.59 ± 0.06). Thalamic regions also increased their overall connectivity to the lentiform nuclei (5 nodes, $r_{avg} \pm$SEM; wake: 0.25 ± 0.02, N1: 0.25 ± 0.02, N2: 0.37 ± 0.15) suggestive of an overall increase in subcortical connectivity in the descent to sleep.

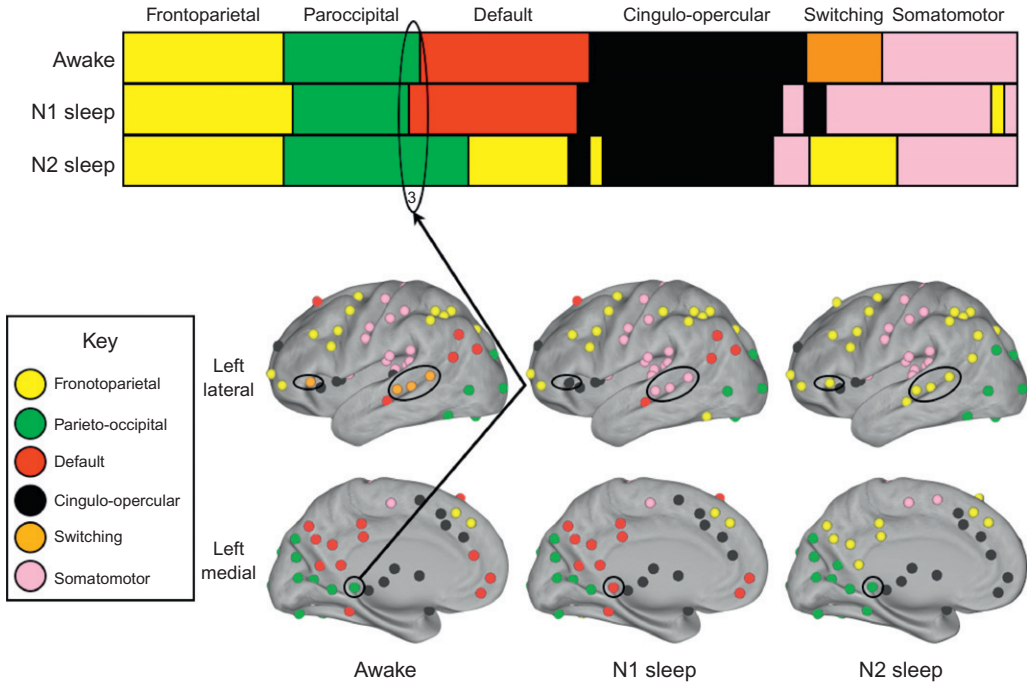

Fig. 5. Summary of changes in network community structure in the state change from wake to N2 sleep. The upper panel plots all 151 nodal regions of interest as a function of their modularity assignment for three neural states: wake, N1, and N2 sleep. Subnetworks are assigned a subnet-specific pattern with network label noted above the panel. Shifts in regional network community assignments are illustrated on CARET maps (left hemisphere only) to indicate their spatial location.

Discussion

Quiet eyes-closed rest has long been associated with posterior alpha-band activity (Berger, 1930). This state predisposes to disengagement from the external world. Recent evidence suggests that such disengagement is associated with enhanced DMN activity (Andrews-Hanna et al., 2010a; Mason et al., 2007), and we report that core elements of the DMN including lateral parietal, medial prefrontal, and PCC are indeed correlated to alpha activity over short scan durations. This has not been a common finding, which may be due to the fact that this correlation is relatively weak (not present at $p < 0.01$, uncorrected). The lack of consensus concerning the correlation of this electrophysiological measure of environmental disengagement is likely due to within state fluctuations in attentional state (Ben-Simon et al., 2008; Davis et al., 1938; Fransson, 2005; Loomis et al., 1937; Olbrich et al., 2009; Vanhaudenhuyse et al., 2010) along with individual differences in brain dynamics (Goncalves et al., 2006).

Over long-duration scans, individuals are more likely to drift into early, N1 sleep. In keeping with previous results (Goldman et al., 2002; Laufs et al., 2006), we see a shift from the broadly frontoparietal pattern of anticorrelated activity in short duration scans to an occipitoparietal pattern in long-duration scans. This pattern is sufficiently strong to survive random effects analysis ($p < 0.01$, uncorrected). A positive correlation to midcingulate regions medially and aI/fOp cortices laterally, that has not been previously reported, was seen to long-duration scans; however, this pattern does not survive random effects analysis

($p < 0.01$, uncorrected). As has been reported by others, positive correlations to thalamus that survive random effects analysis ($p < 0.01$, uncorrected) are present in both short and long-duration scans. The observed pattern of a positive relationship between alpha activity and DMN together with a negative relationship to attentional networks is consistent with the hypothesis that increases in alpha-band power during quiet wake signal a reduction of externally directed attention.

The positive correlations to aI/fOp during long-duration scans is particularly intriguing and bears some relationship to a putative tonic alertness network reported in a recent EEG/fMRI study (Sadaghiani et al., 2010). If, as has been suggested, these regions function as a switch between DMN and networks associated with attention to salient external stimuli (Sridharan et al., 2008), they might also do so during periods in which attention fluctuates between an external and internal focus. Alternatively, since these regions have been reported to be involved in either tonic alertness (Sadaghiani et al., 2010) or attention-related task monitoring (Dosenbach et al., 2006; Nelson et al., 2010; Sridharan et al., 2008) activity in these regions may reflect effort on the part of these subjects to maintain alertness in the face of increasing pressure to fall asleep.

Using seed-based functional connectivity analyses, we report a shift between the negative relationship between DMN and both the DAN (Corbetta and Shulman, 2002; Fox et al., 2006) and an ECN whose core members are part of the cingulo-opercular control network (Dosenbach et al., 2006, 2008). These results are consistent with results reported in behavioral (Mason et al., 2007; Vanhaudenhuyse et al., 2010; Weissman et al., 2006) studies relating mental lapses of attention and mind wandering to increased activity in DMN and neuroimaging studies (Goldman et al., 2002; Kaufmann et al., 2006; Kjaer et al., 2002; Laufs et al., 2006; Moosmann et al., 2003) that note an early reduction in activity in a broad performance-related frontoparietal network that is normally engaged in task-related attentional focus.

Correlations between electrophysiological signals known to change in amplitude in the transition to sleep and the BOLD signal mirror other imaging studies of this transition (Czisch et al., 2004; Horovitz et al., 2008, 2009; Kjaer et al., 2002; Larson-Prior et al., 2009; Picchioni et al., 2008; Sadato et al., 1998; Spoormaker et al., 2010) in suggesting functional reorganization of cortical and thalamic networks with the transition from wake to sleep. The functional connectivity results presented here reflect a reorganization of inter-regional network connectivity in a limited set of attention-related networks. However, these studies were framed in terms of correlations within fixed loci and provide a restricted view of the topography of this reorganization.

To broaden the focus, we examined global network connectivity in this early stage of sleep, finding reorganization in N2 into five locally connected networks (POS, cerebellar, SM, COPs, and FPS) organized roughly as a set of posterior to anterior modules. The appearance of these large local modules was accompanied by the loss of long-range connectivity that is particularly apparent in the dissolution of the anterior–posterior connections of the DMN at the onset of "true" N2 sleep. These results are generally consistent with those recently reported by others (Spoormaker et al., 2010).

Using a graph theoretical approach to the analysis of MEG data across states, Bassett et al. (2006) suggested that a hallmark of small-world brain networks may be adaptive reconfiguration without substantive shifts in global network architecture. Here, we have shown that the initial state change from wake to sleep is accompanied by relatively small shifts in global network architecture largely confined to regional connectors. These data suggest the ability of the global brain network to reconfigure dynamically in relatively higher frequency bands (> 4 Hz) while maintaining a stable architecture over the correlation structure provided by low frequency BOLD oscillations (< 0.1 Hz).

With the descent into early N2, we see a shift in global network architecture that favors both a

strengthening of local over long-range functional connectivity, and coalescence into a more limited set of modules. This pattern has also been reported by others (Spoormaker et al., 2010) but was not clearly seen in more limited investigations of inter-regional connectivity for specific functional networks where internetwork connectivity was reported to be maintained (Horovitz et al., 2009; Larson-Prior et al., 2009). As sleep deepens, however, several studies have reported the dissolution of inter-regional functional connectivity in spatially distributed networks (Horovitz et al., 2009) and large-scale global networks (Spoormaker et al., 2010). In particular, the loss of functional connectivity between anterior and posterior nodes of the DMN, and an increase between posterior regions of DMN has been reported in N3 (Horovitz et al., 2009). We also see an increase in functional connectivity between posterior DMN regions that associate with parahippocampal, parietal, and posterior cingulate regions in N2. Lateral parietal functional connectivity also reconfigured, with wake and N1 state DMN regions joining the FPS in N2. Thus, even in N2, examination of global network architecture indicates a breakdown in long-range functional connectivity that has previously been reported only in N3.

The data reported here point to the importance of assessing state dependent changes in network architecture using global measures rather than simple correlation between isolated regions pairs. Using this wider perspective, we may begin to understand how brain networks maintain their stability during while dynamically reconfiguring during state changes.

Acknowledgments

The authors thank Drs. Fred Prior and Charles Hildebolt for their assistance with the cluster analysis. We thank our funding sources: NS006833 (MER/AZS) and the Mallinckrodt Institute of Radiology.

References

Andrews-Hanna, J. R., Reidler, J. S., Huang, C., & Buckner, R. L. (2010a). Evidence for the default network's role in spontaneous cognition. *Journal of Neurophysiology*, *104*, 322–335.

Andrews-Hanna, J. R., Reidler, J. S., Sepulcre, J., Poulin, R., & Buckner, R. L. (2010b). Functional-anatomic fractionation of the brain's default network. *Neuron*, *65*, 550–562.

Atienza, M., Cantero, J. L., & Escera, C. (2001). Auditory information processing during human sleep as revealed by event-related brain potentials. *Clinical Neurophysiology*, *112*, 2031–2045.

Bachman, D., & Rabins, P. (2006). "Sundowning" and other temporally associated agitation states in dementia patients. *Annual Review of Medicine*, *57*, 499–511.

Bassett, D. S., Meyer-Lindenberg, A., Achard, S., Duke, T., & Bullmore, E. (2006). Adaptive reconfiguration of fractal small-world human brain functional networks. *Proceedings of the National Academy of Sciences*, *103*, 19518–19523.

Beauchamp, M. S., Petit, L., Ellmore, T. M., Ingeholm, J., & Haxby, J. V. (2001). A parametric fMRI study of overt and covert shifts of visuospatial attention. *NeuroImage*, *14*, 310–321.

Bender-Demoll, S., & McFarland, D. A. (2006). The art and science of dynamic network visualization. *Journal of Social Structure*, *7*, 1–46.

Ben-Simon, E., Podlipsky, I., Arieli, A., Zhdanov, A., & Hendler, T. (2008). Never resting brain: Simultaneous representation of two alpha related processes in humans. *PloS ONE*, *3*, e3984.

Berger, H. (1930). Uber das Elektoenkephalogram des Menschen. *Journal für Psychologie und Neurologie*, *40*, 160–179.

Boyton, G. M., Engel, S. A., Glover, G. H., & Heeger, D. J. (1996). Linear systems analysis of functional magnetic resonance imaging in humans. *The Journal of Neuroscience*, *16*, 4207–4221.

Braun, A. R., Balkin, T. J., Wesenten, N. J., Carson, R. E., Varga, M., Baldwin, P., et al. (1997). Regional cerebral blood flow throughout the sleep-wake cycle. An H2(15)O PET study. *Brain*, *120*(Pt 7), 1173–1197.

Bullmore, E., & Sporns, O. (2009). Complex brain networks: Graph theoretical analysis of structural and functional systems. *Nature Reviews. Neuroscience*, *10*, 186–198.

Campbell, S. S., & Murphy, P. J. (2007). The nature of spontaneous sleep across adulthood. *Journal of Sleep Research*, *16*, 24–32.

Cicogna, P. C., Natale, V., Occhionero, M., & Bosinelli, M. (1998). A comparison of mental activity during sleep onset and morning awakening. *Sleep*, *21*, 462–470.

Claassen, D. O., Josephs, K. A., Ahlskog, J. E., Silber, M. H., Tippmann-Peikert, M., & Boeve, B. F. (2010). REM sleep

behavior disorder preceding other aspects of synucleinopathies by up to half a century. *Neurology*, *75*, 494–499.

Corbetta, M., & Shulman, G. L. (2002). Control of goal-directed and stimulus-driven attention in the brain. *Nature Reviews. Neuroscience*, *3*, 201–215.

Corsi-Cabrera, M., Munoz-Torres, Z., Del Rio-Portilla, Y., & Guevara, M. A. (2006). Power and coherent oscillations distinguish REM sleep, stage 1 and wakefulness. *International Journal of Psychophysiology*, *60*, 59–66.

Czisch, M., Wehrle, R., Kaufmann, C., Wetter, T. C., Holsboer, F., Pollmacher, T., et al. (2004). Functional MRI during sleep: BOLD signal decreases and their electrophysiological correlates. *The European Journal of Neuroscience*, *20*, 566–574.

Dang-Vu, T. T., Desseilles, M., Laureys, S., Degueldre, C., Perrin, F., Phillips, C., et al. (2005). Cerebral correlates of delta waves during non-REM sleep revisited. *NeuroImage*, *28*, 14–21.

Dang-Vu, T. T., Schabus, M., Desseilles, M., Albouy, G., Boly, M., Darsaud, A., et al. (2008). Spontaneous neural activity during human slow wave sleep. *Proceedings of the National Academy of Sciences of the United States of America*, *105*, 15160–15165.

Davis, H., Davis, P. A., Loomis, A. L., Harvey, E. N., & Hobart, G. (1938). Human brain potentials during the onset of sleep. *Journal of Neurophysiology*, *1*, 24.

de Gennaro, L., Vecchio, F., Ferrara, M., Curcio, G., Rossini, P. M., & Babiloni, C. (2005). Antero-posterior functional coupling at sleep onset: Changes as a function of increased sleep pressure. *Brain Research Bulletin*, *65*, 133–140.

de Luca, M., Beckmann, C. F., de Stefano, N., Matthews, P. M., & Smith, S. M. (2006). fMRI resting state networks define distinct modes of long-distance interactions in the human brain. *NeuroImage*, *29*, 1359–1367.

de Munck, J. C., Goncalves, S. I., Huijboom, L., Kuijer, J. P., Pouwels, P. J., Heethaar, R. M., et al. (2007). The hemodynamic response of the alpha rhythm: An EEG/fMRI study. *NeuroImage*, *35*, 1142–1151.

Dosenbach, N. U., Fair, D. A., Cohen, A. L., Schlaggar, B. L., & Petersen, S. E. (2008). A dual-networks architecture of top-down control. *Trends in Cognitive Sciences*, *12*, 99–105.

Dosenbach, N. U., Fair, D. A., Miezin, F. M., Cohen, A. L., Wenger, K. K., Dosenbach, R. A., et al. (2007). Distinct brain networks for adaptive and stable task control in humans. *Proceedings of the National Academy of Sciences of the United States of America*, *104*, 11073–11078.

Dosenbach, N. U., Nardos, B., Cohen, A. L., Fair, D. A., Power, J. D., Church, J. A., et al. (2010). Prediction of individual brain maturity using fMRI. *Science*, *329*, 1358–1361.

Dosenbach, N. U., Visscher, K. M., Palmer, E. D., Miezin, F. M., Wenger, K. K., Kang, H. C., et al. (2006). A core system for the implementation of task sets. *Neuron*, *50*, 799–812.

Escandon, A., Al-Hammadi, N., & Galvin, J. E. (2010). Effect of cognitive fluctuation on neuropsychological performance in aging and dementia. *Neurology*, *74*, 210–217.

Esposito, F., Bertolino, A., Scarabino, T., Latorre, V., Blasi, G., Popolizio, T., et al. (2006). Independent component model of the default-mode brain function: Assessing the impact of active thinking. *Brain Research Bulletin*, *70*, 263–269.

Fair, D. A., Cohen, A. L., Power, J. D., Dosenbach, N. U., Church, J. A., Miezin, F. M., et al. (2009). Functional brain networks develop from a "local to distributed" organization. *PLoS Computational Biology*, *5*, e1000381.

Fair, D. A., Dosenbach, N. U., Church, J. A., Cohen, A. L., Brahmbhatt, S., Miezin, F. M., et al. (2007). Development of distinct control networks through segregation and integration. *Proceedings of the National Academy of Sciences of the United States of America*, *104*, 13507–13512.

Feige, B., Scheffler, K., Esposito, F., di Salle, F., Hennig, J., & Seifritz, E. (2005). Cortical and subcortical correlates of electroencephalographic alpha rhythm modulation. *Journal of Neurophysiology*, *93*, 2864–2872.

Fox, M. D., Corbetta, M., Snyder, A. Z., Vincent, J. L., & Raichle, M. E. (2006). Spontaneous neuronal activity distinguishes human dorsal and ventral attention systems. *Proceedings of the National Academy of Sciences of the United States of America*, *103*, 10046–10051.

Fox, M. D., Snyder, A. Z., Vincent, J. L., Corbetta, M., van Essen, D. C., & Raichle, M. E. (2005). The human brain is intrinsically organized into dynamic, anticorrelated functional networks. *Proceedings of the National Academy of Sciences*, *102*, 9673–9678.

Fransson, P. (2005). Spontaneous low-frequency BOLD signal fluctuations: An fMRI investigation of the resting-state default mode of brain function hypothesis. *Human Brain Mapping*, *26*, 15–29.

Gertner, S., Greenbaum, C. W., Sadeh, A., Dolfin, Z., Sirota, L., & Ben-Nun, Y. (2002). Sleep-wake patterns in preterm infants and 6 month's home environment: Implications for early cognitive development. *Early Human Development*, *68*, 93–102.

Goldman, R. I., Stern, J. M., Engel, J., JR.& Cohen, M. S. (2002). Simultaneous EEG and fMRI of the alpha rhythm. *Neuroreport*, *13*, 2487–2492.

Goncalves, S. I., de Munck, J. C., Pouwels, P. J., Schoonhoven, R., Kuijer, J. P., Maurits, N. M., et al. (2006). Correlating the alpha rhythm to BOLD using simultaneous EEG/fMRI: Inter-subject variability. *NeuroImage*, *30*, 203–213.

Gusnard, D. A., Akbudak, E., Shulman, G. L., & Raichle, M. E. (2001). Medial prefrontal cortex and self-referential mental activity: Relation to a default mode of brain function. *Proceedings of the National Academy of Sciences of the United States of America*, *98*, 4259–4264.

He, B. J., Snyder, A. Z., Zempel, J. M., Smyth, M. D., & Raichle, M. E. (2008). Electrophysiological correlates of the brain's intrinsic large-scale functional architecture. *Proceedings of the National Academy of Sciences of the United States of America*, *105*, 16039–16044.

Horovitz, S. G., Braun, A. R., Carr, W. S., Picchioni, D., Balkin, T. J., Fukunaga, M., et al. (2009). Decoupling of the brain's default mode network during deep sleep. *Proceedings of the National Academy of Sciences of the United States of America*, *106*, 11376–11381.

Horovitz, S. G., Fukunaga, M., de Zwart, J. A., van Gelderen, P., Fulton, S. C., Balkin, T. J., et al. (2008). Low frequency BOLD fluctuations during resting wakefulness and light sleep: A simultaneous EEG-fMRI study. *Human Brain Mapping*, *29*, 671–682.

Humphries, M. D., & Gurney, K. (2008). Network 'small-world-ness': A quantitative method for determining canonical network equivalence. *PloS ONE*, *3*, e0002051.

Iber, C., Ancoli-Israel, S., Chesson, A. L. J., & Quan, S. F. (2007). *The AASM manual for the scoring of sleep and associated events.* Westchester, IL: American Academy of Sleep Medicine.

Jann, K., Dierks, T., Boesch, C., Kottlow, M., Strik, W., & Koenig, T. (2009). BOLD correlates of EEG alpha phase-locking and the fMRI default mode network. *NeuroImage*, *45*, 903–916.

Kaufmann, C., Wehrle, R., Wetter, T. C., Holsboer, F., Auer, D. P., Pollmacher, T., et al. (2006). Brain activation and hypothalamic functional connectivity during human non-rapid eye movement sleep: An EEG/fMRI study. *Brain*, *129*, 655–667.

Kjaer, T. W., Law, I., Wiltschiotz, G., Paulson, O. B., & Madsen, P. L. (2002). Regional cerebral blood flow during light sleep–a H(2)(15)O-PET study. *Journal of Sleep Research*, *11*, 201–207.

Lancichinetti, A., Kivela, M., Saramaki, J., & Fortunato, S. (2010). Characterizing the community structure of complex networks. *PloS ONE*, *5*, e11976.

Larson-Prior, L. J., Zempel, J. M., Nolan, T. S., Prior, F. W., Snyder, A. Z., & Raichle, M. E. (2009). Cortical network functional connectivity in the descent to sleep. *Proceedings of the National Academy of Sciences of the United States of America*, *106*, 4489–4494.

Laufs, H., Holt, J. L., Elfont, R., Krams, M., Paul, J. S., Krakow, K., et al. (2006). Where the BOLD signal goes when alpha EEG leaves. *NeuroImage*, *31*, 1408–1418.

Laufs, H., Kleinschmidt, A., Beyerle, A., Eger, E., Salek-Haddadi, A., Preibisch, C., et al. (2003a). EEG-correlated fMRI of human alpha activity. *NeuroImage*, *19*, 1463–1476.

Laufs, H., Krakow, K., Sterzer, P., Eger, E., Beyerle, A., Salek-Haddadi, A., et al. (2003b). Electroencephalographic signatures of attentional and cognitive default modes in spontaneous brain activity fluctuations at rest. *Proceedings of the National Academy of Sciences of the United States of America*, *100*, 11053–11058.

Loomis, A. L., Harvey, E. N., & Hobart, G. A. (1937). Cerebral states during sleep, as studied by human brain potentials. *Journal of Experimental Psychology*, *21*, 127–144.

Magnin, M., Bastuji, H., Garcia-Larrea, L., & Mauguiere, F. (2004). Human thalamic medial pulvinar nucleus is not activated during paradoxical sleep. *Cerebral Cortex*, *14*, 858–862.

Maquet, P., Peters, J., Aerts, J., Delfiore, G., Degueldre, C., Luxen, A., et al. (1996). Functional neuroanatomy of human rapid-eye-movement sleep and dreaming. *Nature*, *383*, 163–166.

Maquet, P., Ruby, P., Maudoux, A., Albouy, G., Sterpenich, V., Dang-Vu, T., et al. (2005). Human cognition during REM sleep and the activity profile within frontal and parietal cortices: A reappraisal of functional neuroimaging data. *Progress in Brain Research*, *150*, 219–227.

Mason, M. F., Norton, M. I., van Horn, J. D., Wegner, D. M., Grafton, S. T., & Macrae, C. N. (2007). Wandering minds: The default network and stimulus-independent thought. *Science*, *315*, 393–395.

Merica, H., & Fortune, R. D. (2004). State transitions between wake and sleep, and within the ultradian cycle, with focus on the link to neuronal activity. *Sleep Medicine Reviews*, *8*, 473–485.

Moller, J. C., Unger, M., Stiasny-Kolster, K., Kaussner, Y., Penzel, T., Oertel, W. H., et al. (2009). Continuous sleep EEG monitoring in PD patients with and without sleep attacks. *Parkinsonism & Related Disorders*, *15*, 238–241.

Moosmann, M., Ritter, P., Krastel, I., Brink, A., Thees, S., Blankenburg, F., et al. (2003). Correlates of alpha rhythm in functional magnetic resonance imaging and near infrared spectroscopy. *NeuroImage*, *20*, 145–158.

Munch, M., Silva, E. J., Ronda, J. M., Czeisler, C. A., & Duffy, J. F. (2010). EEG sleep spectra in older adults across all circadian phases during NREM sleep. *Sleep*, *33*, 389–401.

Nelson, S. M., Cohen, A. L., Power, J. D., Wig, G. S., Miezin, F. M., Wheeler, M. E., et al. (2010). A parcellation scheme for human left lateral parietal cortex. *Neuron*, *67*, 156–170.

Newman, M. E. (2006). Modularity and community structure in networks. *Proceedings of the National Academy of Sciences of the United States of America*, *103*, 8577–8582.

Nofzinger, E. A., Buysse, D. J., Miewald, J. M., Meltzer, C. C., Price, J. C., Sembrat, R. C., et al. (2002). Human regional cerebral glucose metabolism during non-rapid eye movement sleep in relation to waking. *Brain*, *125*, 1105–1115.

Ogilvie, R. D. (2001). The process of falling asleep. *Sleep Medicine Reviews*, *5*, 247–270.

Ojemann, J. G., Akbudak, E., Snyder, A. Z., McKinstry, R. C., Raichle, M. E., & Conturo, T. E. (1997). Anatomic localization and quantitative analysis of gradient refocused echo-planar fMRI susceptibility artifacts. *NeuroImage*, *6*, 156–167.

Olbrich, S., Mulert, C., Karch, S., Trenner, M., Leicht, G., Pogarell, O., et al. (2009). EEG-vigilance and BOLD effect during simultaneous EEG/fMRI measurement. *NeuroImage*, *45*, 319–332.

Picchioni, D., Fukunaga, M., Carr, W. S., Braun, A. R., Balkin, T. J., Duyn, J. H., et al. (2008). fMRI differences between early and late stage-1 sleep. *Neuroscience Letters*, *441*, 81–85.

Portas, C. M., Krakow, K., Allen, P., Josephs, O., Armony, J. L., & Frith, C. D. (2000). Auditory processing across the sleep-wake cycle: Simultaneous EEG and fMRI monitoring in humans. *Neuron*, *28*, 991–999.

Power, J. D., Cohen, A. L., Nelson, S. M., Wig, G. S., Miezin, F. M., Vogel, A. C., et al. (2010a). *The network architecture of functionally defined regions spanning the brain reorganize from a predominantly local architecture in children to a distributed, functional architecture in adults.* Montreal, QC, Canada: Cognitive Neuroscience Society.

Power, J. D., Fair, D. A., Schlaggar, B. L., & Petersen, S. E. (2010b). The development of human functional brain networks. *Neuron*, *67*, 735–748.

Rechtshaffen, A., & Kales, A. (1968). *A manual of standardized terminology, techniques, and scoring system for sleep stages of human subjects.* Los Angeles: Brain Information Service/Brain Research Inst., UCLA.

Roth, B. (1961). The clinical and theoretical importance of EEG rhythms corresponding to states of lowered vigilance. *Electroencephalography and Clinical Neurophysiology*, *13*, 395–399.

Rowley, J. T., Stickgold, R., & Hobson, J. A. (1998). Eyelid movements and mental activity at sleep onset. *Consciousness and Cognition*, *7*, 67–84.

Sadaghiani, S., Scheeringa, R., Lehongre, K., Morillon, B., Giraud, A. L., & Kleinschmidt, A. (2010). Intrinsic connectivity networks, alpha oscillations, and tonic alertness: A simultaneous electroencephalography/functional magnetic resonance imaging study. *The Journal of Neuroscience*, *30*, 10243–10250.

Sadato, N., Nakamura, S., Oohashi, T., Nishina, E., Fuwamoto, Y., Waki, A., et al. (1998). Neural networks for generation and suppression of alpha rhythm: A PET study. *Neuroreport*, *9*, 893–897.

Song, Y., Dowling, G. A., Wallhagen, M. I., Lee, K. A., & Strawbridge, W. J. (2010). Sleep in older adults with Alzheimer's disease. *The Journal of Neuroscience Nursing*, *42*, 190–198 quiz 199–200.

Spoormaker, V. L., Schroter, M. S., Gleiser, P. M., Andrade, K. C., Dresler, M., Wehrle, R., et al. (2010). Development of a large-scale functional brain network during human non-rapid eye movement sleep. *The Journal of Neuroscience*, *30*, 11379–11387.

Sridharan, D., Levitin, D. J., & Menon, V. (2008). A critical role for the right fronto-insular cortex in switching between central-executive and default-mode networks. *Proceedings of the National Academy of Sciences of the United States of America*, *105*, 12569–12574.

Terry, J. R., Anderson, C., & Horne, J. A. (2004). Nonlinear analysis of EEG during NREM sleep reveals changes in functional connectivity due to natural aging. *Human Brain Mapping*, *23*, 73–84.

Tyvaert, L., Levan, P., Grova, C., Dubeau, F., & Gotman, J. (2008). Effects of fluctuating physiological rhythms during prolonged EEG-fMRI studies. *Clinical Neurophysiology*, *119*, 2762–2774.

van Essen, D. C. (2005). A population-average, landmark- and surface-based (PALS) atlas of human cerebral cortex. *NeuroImage*, *28*, 635–662.

van Essen, D. C., Drury, H. A., Dickson, J., Harwell, J., Hanlon, D., & Anderson, C. H. (2001). An integrated software suite for surface-based analyses of cerebral cortex. *Journal of the American Medical Informatics Association*, *8*, 443–459.

Vanhaudenhuyse, A., Demertzi, A., Schabus, M., Noirhomme, Q., Bredart, S., Boly, M., et al. (2010). Two distinct neuronal networks mediate the awareness of environment and of self. *Journal of Cognitive Neuroscience*, 1–9.

Vincent, J. L., Larson-Prior, L. J., Zempel, J. M., & Snyder, A. Z. (2007). Moving GLM ballistocardiogram artifact reduction for EEG acquired simultaneously with fMRI. *Clinical Neurophysiology*, *118*, 981–998.

Vincent, J. L., Kahn, I., Snyder, A. Z., Raichle, M. E., & Buckner, R. L. (2008). Evidence for a frontoparietal control system revealed by intrinsic functional connectivity. *Journal of Neurophysiology*, *100*, 3328–3342.

Walters, A. S., Silvestri, R., Zucconi, M., Chandrashekariah, R., & Konofal, E. (2008). Review of the possible relationship and hypothetical links between attention deficit hyperactivity disorder (ADHD) and the simple sleep related movement disorders, parasomnias, hypersomnias, and circadian rhythm disorders. *Journal of Clinical Sleep Medicine*, *4*, 591–600.

Watts, D. J., & Strogatz, S. H. (1998). Collective dynamics of 'small-world' networks. *Nature*, *393*, 440–442.

Wehrle, R., Czisch, M., Kaufmann, C., Wetter, T. C., Holsboer, F., Auer, D. P., et al. (2005). Rapid eye movement-related brain activation in human sleep: A functional magnetic resonance imaging study. *Neuroreport*, *16*, 853–857.

Wehrle, R., Kaufmann, C., Wetter, T. C., Holsboer, F., Auer, D. P., Pollmacher, T., et al. (2007). Functional microstates within human REM sleep: First evidence from fMRI of a thalamocortical network specific for phasic REM periods. *The European Journal of Neuroscience*, *25*, 863–871.

Weissman, D. H., Roberts, K. C., Visscher, K. M., & Woldorff, M. G. (2006). The neural bases of momentary lapses in attention. *Nature Neuroscience*, *9*, 971–978.

Yang, C. M., Han, H. Y., Yang, M. H., Su, W. C., & Lane, T. (2010). What subjective experiences determine the perception of falling asleep during sleep onset period? *Consciousness and Cognition*, *19*, 1084–1092.

Zorick, F., Roehrs, T., Wittig, R., Lamphere, J., Sicklesteel, J., & Roth, T. (1986). Sleep-wake abnormalities in narcolepsy. *Sleep*, *9*, 189–193.